

# WIDEBAND RADIO CHANNEL VARIATION WITH INDOOR TERMINAL SEPARATION: MEASUREMENT RESULTS

D. Porrat\* and Y. Serfaty

*The Hebrew University of Jerusalem*

*Jerusalem, Israel 91904*

dporrat@cs.huji.ac.il, yuval.ser@gmail.com

## I. INTRODUCTION

The Multiband OFDM Alliance (MBOA), established to formulate an industry-based standard for UWB communications, suggested dividing the 3-10 GHz spectrum to 14 sub-bands. Motivated by the sub-band approach, this paper presents measurement results of the mean (excess) delay and RMS delay spread. We also analyze channel gain vs. terminal separation and frequency. We characterize the dependence of the measured parameters on the transmitter-receiver separation, in office building settings with no line of sight, our investigation of the dependence of the parameters on sub-carrier frequency did not yield a significant trend of the parameter values vs. carrier frequency. This paper uses the MBOA defined sub-bands with carrier frequencies between 3.432 GHz and 10.296 GHz and 528 MHz bandwidth. Our measurement included terminal separations of 5 - 30 meters.

## II. MEASUREMENTS

### A. *Equipment*

The measurement setup was based on an Agilent N5230 network analyzer, connected to two omni-directional antennas (Electro-Metrics EM-6865) with suitable amplifiers. Measurements were swept over the 1-18 GHz range, with a frequency resolution of 10.6 MHz (16001 point per sweep). The antennas were placed on carts that were moved to different locations for different measurements, and were immobile during each measurement. A computer controlled the location of the receiving antenna over a rail, as well as the parameters of the network analyzer and the data collection, that was lengthy since we tried to achieve a high signal to noise ratio over a wide band and used a 50 Hz IF bandwidth. The equipment is further described in the laboratory website at <http://www.cs.huji.ac.il/~dporrat/lab.html>.

### B. *The Measurement Environment*

The 42 measurements analyzed in this paper were collected during 2006–2008 in three buildings in the Givat Ram Campus of the Hebrew University in Jerusalem, two were conventional office building built during the 1960s, of reinforced concrete and concrete blocks, and the third was built during the 2000s, with plasterboard interior walls. The transmitter and receiver were located in the same floor and in adjacent floors. Most of the measurements were taken during nights in order to minimize the effect of movement of people.

This research was supported by the Israel Science Foundation (Grant No. 249/06), and by the Israeli Consortium of Short Range Communications. A similar paper was submitted to PIMRC'08.

### III. METHODS

The results presented below are based on a single impulse response per transmitter and receiver cart position, out of the many measurements taken with different receiver positions along a rail. We do not use multiple measurements with the same transmitter and receiver cart locations because the parameter we calculated were normally stable over the rail. Our impulse response data were obtained by transforming the sampled frequency domain measurements, after linear smoothing in 1 GHz - 2.06 GHz band and zero padding in the 0-1 GHz range [2]. The effective band is 2-18 GHz and the temporal resolution of the full-band data is  $\Delta t_{FB} = 58.8$  psec.

We analyze the channel gain in Section IV-A vs. terminal separation and frequency. After smoothing and transforming the data to the time domain, we trim it (i.e. limit the time domain of interest) at a level that is mbox-25 dB below the maximum, in order to avoid processing noise. The trimming is done by determining the minimal and maximal delay values where the response crosses the threshold, and considering the response only between these two delay values. The sensitivity of RMS delay spread calculated from measurements to the threshold level is discussed in [11]. Our threshold of mbox-25 dB agrees with the SNR available in all our measurements.

The next processing step involves normalizing the (squared and trimmed) impulse response into a power delay profile, i.e. a positive function with a unit integral. The power delay profile is marked  $\{p_n\}$  where  $n$  indicates the temporal (delay) index.

We consider two time spread measures: The mean (excess) delay in Section IV-B and the RMS delay spread in Section IV-C. The mean delay  $\tau_m$  and the RMS delay spread  $\tau_{\text{RMS}}$  are calculated by a discrete (sum) approximation of the standard definition:

$$\tau_m = \sum_{n=1}^{\infty} n p_n \Delta t \quad (1)$$

$$\tau_{\text{RMS}} = \sum_{n=1}^{\infty} (n - \tau_m)^2 p_n \Delta t \quad (2)$$

The exponential decay rate is calculated by fitting our measurements to a single exponential, following [12] and others. We perform a weighted minimum mean square error fit to the log-PDP, i.e.  $\ln p_n$ , with the weights  $p_n$ , minimizing the following sum over the two parameters  $\tau_e$  and  $a$ :

$$\sum \left( \ln(p_n) - \left( -\frac{n\Delta t}{\tau_e} + a \right) \right)^2 p_n \quad (3)$$

to obtain the decay rate  $\tau_e$ . The sum (3) is taken from the delay of the maximum of the response  $\{p_n\}$  to the end of its temporal axis.

To clarify the processing we consider the parameter *par* that stands for the mean delay, the RMS delay spread, the exponential decay rate and the number of significant taps in different parts of the text. We start with 588 values of the parameter *par*, calculated from 42 terminal locations and 14 sub-bands per location.

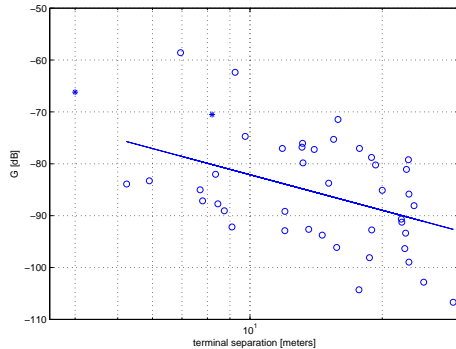


Fig. 1. The channel gain vs. terminal separation in a log-log graph. The linear fit is given by  $G^l(d) \sim d[\text{m}]^{-2.3}$ . The stars indicate results from [9]:  $L=-66.2$  dB for  $d=4$  m and  $L=-70.5$  dB for  $d=8.2$  m (Table 1 and Figure 4), these two measurements may be close to LoS.

Averaging over the sub-carrier frequency yields the best linear approximation of the form  $par(d) \approx \text{const } d + \text{const}$ , where  $d$  stands for terminal (antenna) separation in meters. Linear fits of this type are presented in Figures 2 and 4, along with the related mean square error (MSE) values.

Analysis then proceeds to the correlation of each parameter across sub-bands. To calculate the correlation we subtract the separation dependent linear trend from the parameter values, and use the resulting zero-mean values to calculate the variance and the correlation between the parameter values across different sub-bands. The correlation coefficient vs. sub-band carrier separation is plotted in Figures 3 and 5 along with the best (minimum MSE) linear fit.

## IV. RESULTS

### A. Path Loss

We plot the path loss (channel gain) in a logarithmic (dB) scale vs. log terminal separation. A straight line with slope  $n$  in this representation indicates a power connection between the terminal separation  $d$  and the received power  $G$ :  $G \sim d^{-n}$ . This type of connection is the common model for mean path loss dependence on terminal separation. The parameter  $n$  is often termed ‘path loss exponent’.

The linear fit of Figure 1 gives a path loss exponent of -2.3. [6] show in their Figure 9 path loss exponent results of 1.96 for NLoS. [2] find path loss exponents that range from 3.04 at a carrier frequency of 3.15 GHz, an exponent of 2.92 at a carrier frequency of 5.6 GHz and 4.1 at 7.95 GHz, with a bandwidth of 100 MHz.

After fitting the gain vs. frequency plot to a linear approximation and averaging over our measurements, we found that the average linear frequency dependence of the gain is given by -1.25 dB/GHz. We note that [3] find a slope of about 15.3 dB/GHz for a single NLoS measurement (calculated from Figure 12 there). [9] find slopes of 50 dB/GHz and 60 dB/GHz for NLoS measurements with terminal separations of 4 m and 8.2 m, with a single wall (of an unspecified type) separating the terminals, over the band 2-6 GHz. The large range of results calls for verification by a thorough study.

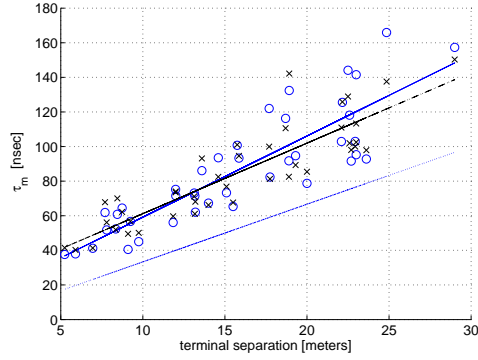


Fig. 2. Mean (excess) delay vs. terminal separation. The circles and full line show sub-band results averages over the 14 sub-bands. The Xs and dashed line show full band results, and the dotted line shows free space delays calculated from the terminal separation. The free space slope equals  $1/c = 3.33$  nsec/m. The linear fit of the sub-band data (full line) is given by  $\tau_m^{SB}(d)[\text{nsec}] = 4.7 d[\text{m}] + 12.2$  and the full band best fit is  $\tau_m^{FB}(d)[\text{nsec}] = 4.1 d[\text{m}] + 20.4$ . The corresponding MSE are 13.8 nsec for the sub-band data and 11.0 nsec for the full-band data.

[6] consider (in (4)) a frequency dependence of the form

$$G [\text{dB}] = 20 \log_{10} d - 20m \log_{10} f [\text{GHz}] \quad (4)$$

( $d$  does not indicate distance here), for NLoS the average parameters they suggest are  $20 \log_{10} d \approx -55$  dB and  $m = 1.1$  (Figure 8 there).

### B. Mean Delay

Figure 2 shows the mean delay vs. terminal separation. The per-band mean delay is similar to the delay measured over the entire (16 GHz) band, contrary to results from [2] that show a higher per-band mean delay. The best fit linear trend of the per band mean delay is given by

$$\tau_v^{SB}(d) [\text{nsec}] = 4.7d [\text{m}] + 12.2 \quad (5)$$

with a mean square error of 13.8 nsec. and the full-band fit is  $\tau_v^{FB}(d) [\text{nsec}] = 4.1d [\text{m}] + 20.4$ .

The mean delay values calculated over adjacent sub-bands are correlated as seen in Figure 3.

### C. RMS Delay Spread

Figure 4 shows the averaged sub-band RMS delay spread as well as the full band RMS delay spread, vs. terminal separation. The best linear fit of the sub-band data is  $\tau_{\text{RMS}}^{SB}(d)[\text{nsec}] = 0.7 d[\text{m}] + 16.7$ , with a mean square error of 8.8 nsec. The correlation coefficient of the RMS delay spread across sub-bands is closely matched by a linear fit:  $R_{\text{RMS}} = -0.066\Delta f[\text{GHz}] + 0.79$ .

The RMS delay spread values calculated over adjacent sub-bands are correlated as seen in Figure 5.

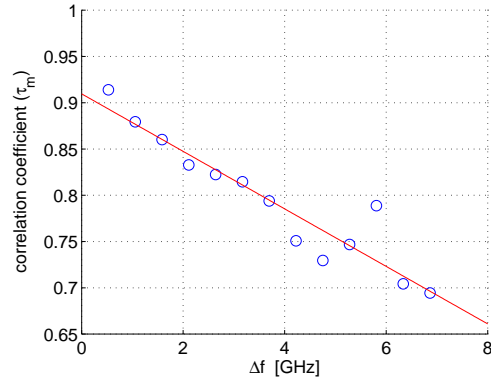


Fig. 3. Mean delay correlation across sub-bands, the linear fit is given by  $R_{\tau_m} = -0.031\Delta f[GHz] + 0.91$ .

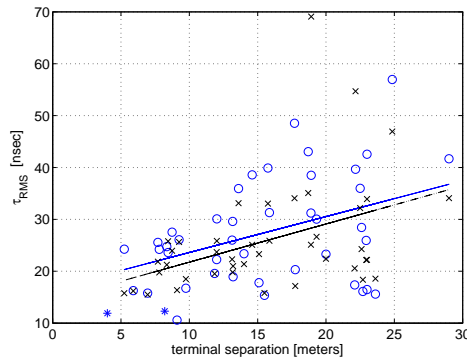


Fig. 4. RMS delay spread vs. terminal separation. The circles and full line show sub-band results averages over the 14 sub-bands. The Xs and dashed line show full band results. The linear fit of the sub-band data (full line) is given by  $\tau_{RMS}^{SB}(d)[nsec] = 0.7 d[m] + 16.7$  (with MSE=8.8 nsec), and the full band data fit is  $\tau_{RMS}^{FB}(d)[nsec] = 0.7 d[m] + 14.4$  (with MSE=6.7 nsec). The stars indicate results from [9] (Table 1 there):  $\tau_{rms} = 11.9$  nsec for  $d = 4$  m and 12.3 nsec for  $d = 8.2$  m.

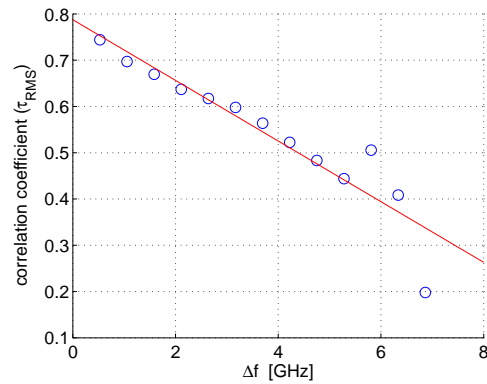


Fig. 5. RMS delay spread correlation across sub-bands, the linear fit is given by  $R_{\tau_{RMS}} = -0.066\Delta f[GHz] + 0.79$ .

[2] present RMS delay spread values averaged over measurements with unspecified terminal separations that appear between 6 m and 13 m from the floor plan in their Figure 2. They find RMS delay spreads of 18 nsec, 17 nsec and 16 nsec for 100 MHz sub-band around 3.15 GHz, 5.6 GHz and 7.95 GHz for mild NLoS conditions. For extreme NLoS conditions they find RMS delay spread values of 21 nsec, 26 nsec and 43 nsec with carrier frequencies of 3.15 GHz, 5.6 GHz and 7.95 GHz. Results in [2] were calculated by thresholding the power delay profile 15 dB above the noise level, that corresponds to 45 dB from the peak in their measurements, where as our threshold was fixed by -25 dB from the temporal peak. See [11] for a demonstration of the sensitivity of the RMS delay spread to the threshold.

## REFERENCES

- [1] S. S. Ghassemzadeh, L. J. Greenstain, T. Sveinsson, A. Kavčić, and V. Tarokh, "UWB delay profile models for residential and commercial indoor environments," *IEEE Transactions on Vehicular Technology*, vol. 54, no. 4, pp. 1235–1244, Jul 2005.
- [2] L. Hentilä, V. Hovinen, and M. Hämäläinen, "Sub-band analysis in UWB radio channel modeling," in *Nordic Radio Symposium/Finnish Wireless Communications Workshop (NRS/FWCW '04)*, Aug 2004, pp. 1–5.
- [3] T. Jämsä, V. Hovinen, A. Karjalainen, and J. Iinatti, "Frequency dependency of delay spread and path loss in indoor ultra-wideband channels," in *Ultra Wideband Systems, Technologies and Applications*. IEEE, Apr 2006, pp. 254–258.
- [4] J. Keignart and N. Daniele, "Subnanosecond UWB channel sounding in frequency and temporal domain," in *Ultra Wideband Systems and Technologies*. IEEE, May 2002, pp. 25–30.
- [5] I. Z. Kovács and P. C. Eggers, "Short-range UWB radio propagation investigations using small terminal antennas," in *International Workshop on Ultra Wideband Systems*, Jun 2003.
- [6] J. Kunisch and J. Pamp, "Measurement results and modeling aspects for the UWB radio channel," in *Ultra Wideband Systems and Technologies*. IEEE, May 2002, pp. 19–23.
- [7] —, "An ultra-wideband space-variant multipath indoor radio channel model," in *Ultra Wideband Systems and Technologies*. IEEE, Nov 2003, pp. 290–294.
- [8] U. Schuster and H. Bölcskei, "Ultrawideband channel modeling on the basis of information-theoretic criteria," *IEEE Transactions on Wireless Communications*, vol. 6, no. 7, pp. 2464–2475, Jul 2007.
- [9] J. Jemai, P. Eggers, G. F. Pedersen, and T. Kürner, "On the applicability of deterministic modelling to indoor UWB channels," in *The 3rd Workshop on Positioning, Navigation and Communication (WPNC)*, 2006.
- [10] J. Foerster, M. Pendergrass, and A. F. Molisch, "A channel model for ultrawideband indoor communication," Nov 2003, mitsubishi Electric Research Laboratory, Inc., TR-2003-73.
- [11] Z. Bodnár, Z. Herczku, and I. Friges, "Noise threshold dependency of the RMS delay spread in wideband measurements of radio propagation channels," in *Telecommunications Symposium (ITS)*. SBT/IEEE, Aug 1998, pp. 312–317.
- [12] D. Cassioli, M. Z. Win, and A. F. Molisch, "The ultra-wide bandwidth indoor channel: from statistical model to simulations," *IEEE Journal on Selected Areas in Communications*, vol. 20, no. 6, pp. 1247–1257, Aug 2002.